This is a repository copy of *Meteorological effects and impacts of the 10 June 2021 solar eclipse over the British Isles, Iceland and Greenland*.

White Rose Research Online URL for this paper:
https://eprints.whiterose.ac.uk/184988/

Version: Published Version

Meteorological effects and impacts of the 10 June 2021 solar eclipse over the British Isles, Iceland and Greenland

**Edward Hanna[1],
Karen Aplin[2] , Halldor
Bjornsson[3], Robert G.
Bryant[4], John Cappelen[5],
Robert Fausto[6], Xavier
Fettweis[7] , Edward
Graham[8], R. Giles
Harrison[9] , Trausti
Jonsson[3], John Penman[10],
Dilkushi de Alwis Pitts[1]
and Alexander J. Bilton[1]**

[1]Department of Geography and Lincoln Climate Research Group, University of Lincoln, Lincoln, UK

[2]Faculty of Engineering, University of Bristol, Bristol, UK

[3]Icelandic Meteorological Office, Reykjavik, Iceland

[4]Department of Geography, University of Sheffield, Sheffield, UK

[5]Danish Meteorological Institute, Copenhagen, Denmark

[6]Geological Survey of Denmark and Greenland, Copenhagen, Denmark

[7]Department of Geography, SPHERES research unit, University of Liège, Liège, Belgium

[8]University of the Highlands and Islands, Stornoway, UK

[9]Department of Meteorology, University of Reading, Reading, UK

[10]Met Office, Edinburgh, UK

Introduction

Solar eclipses have a distinct impact on local- to regional-scale meteorology near Earth's surface, and these effects of total eclipses of the last 10–20 years or so have been widely studied (e.g. Aplin *et al.*, 2016). The typical response involves surface cooling and associated reduced wind speeds, possibly also with some dissipation of convective-type cloud cover, due to reduced mixing in the near-surface atmospheric boundary layer (e.g. Hanna, 2000). For a summary of meteorological studies during previous eclipses, the reader is referred to papers in the special edited volume by Harrison and Hanna (2016), with two widely studied relatively recent events being the total solar eclipses of 11 August 1999 (Hanna, 2000; Aplin and Harrison, 2003) and 20 March 2015 (Hanna *et al.*, 2016; Hanna, 2018). However, most previous work has focused on effects in or near the zone of totality, while relatively few studies have targeted partial solar eclipses, despite the larger area in the partial zone.

Here we analyse data from the British Isles, Iceland and Greenland to investigate potential meteorological effects arising from the partial solar eclipse of 10 June 2021. The eclipse was annular (~94% maximum eclipse magnitude) in a narrow zone over northwest Greenland, while maximum obscuration of the Sun over the British Isles was modest at about 25–45% (Figure 1). Annular eclipses are those where the Moon is too far away to fully cover the Sun at mid-eclipse, with observers in the annular zone seeing a so-called 'ring of fire' around the eclipsed Sun. All times are given
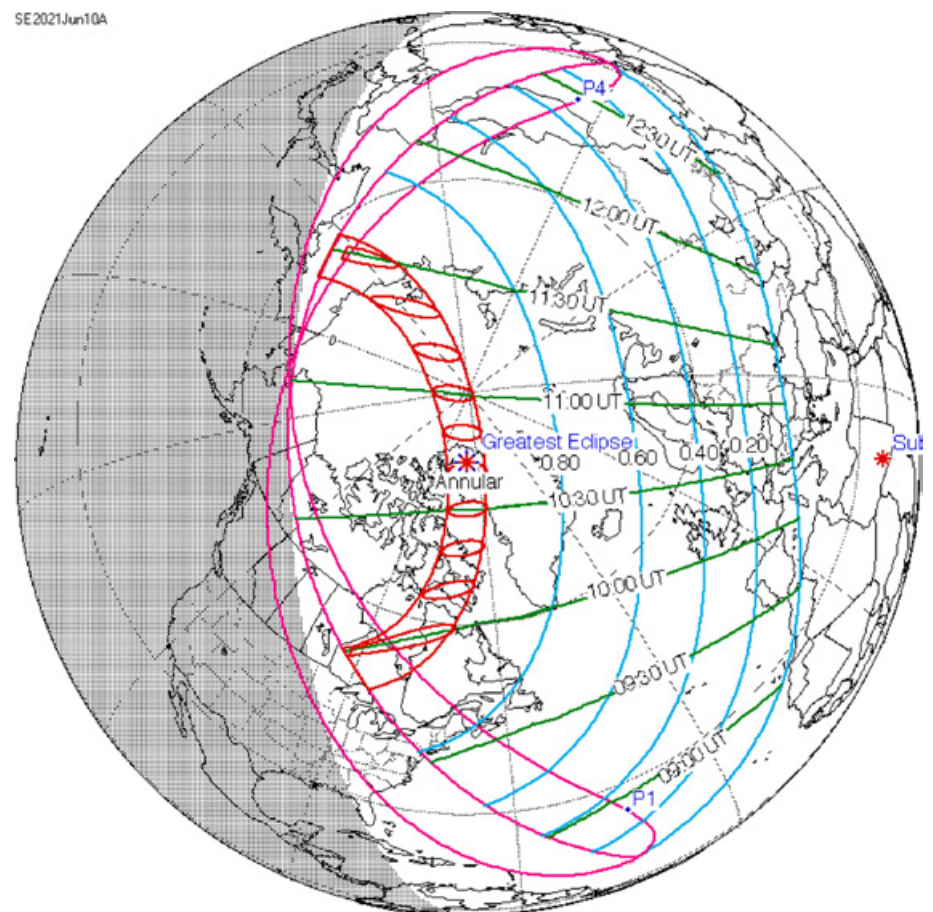
Figure 1. Map showing path and coverage/timing details of the 10 June 2021 partial/annular solar eclipse over the study regions. Green lines indicate local times of greatest eclipse, and blue lines show greatest eclipse magnitude. The eclipse was annular in the red zone but was nowhere total. The larger zone in cerise in an approximate horseshoe shape shows where the eclipse was only marginally visible (cloud permitting) around the time of sunrise or sunset.[1]

RMetS
Royal Meteorological Society

Figure 2. Met Office North Atlantic and European synoptic chart[2] for 0000 UTC on 10 June 2021.

in Coordinated Universal Time (UTC = GMT). In Birmingham (UK), given as a relatively central location for the British Isles, the eclipse started at 0906 UTC, peaked at 1012 UTC and ended at 1123 UTC. The eclipse timings were very similar for Reykjavik (Iceland), where the eclipse started at 0906 UTC, peaked at 1017 UTC and ended at 1132 UTC. In Greenland (except the extr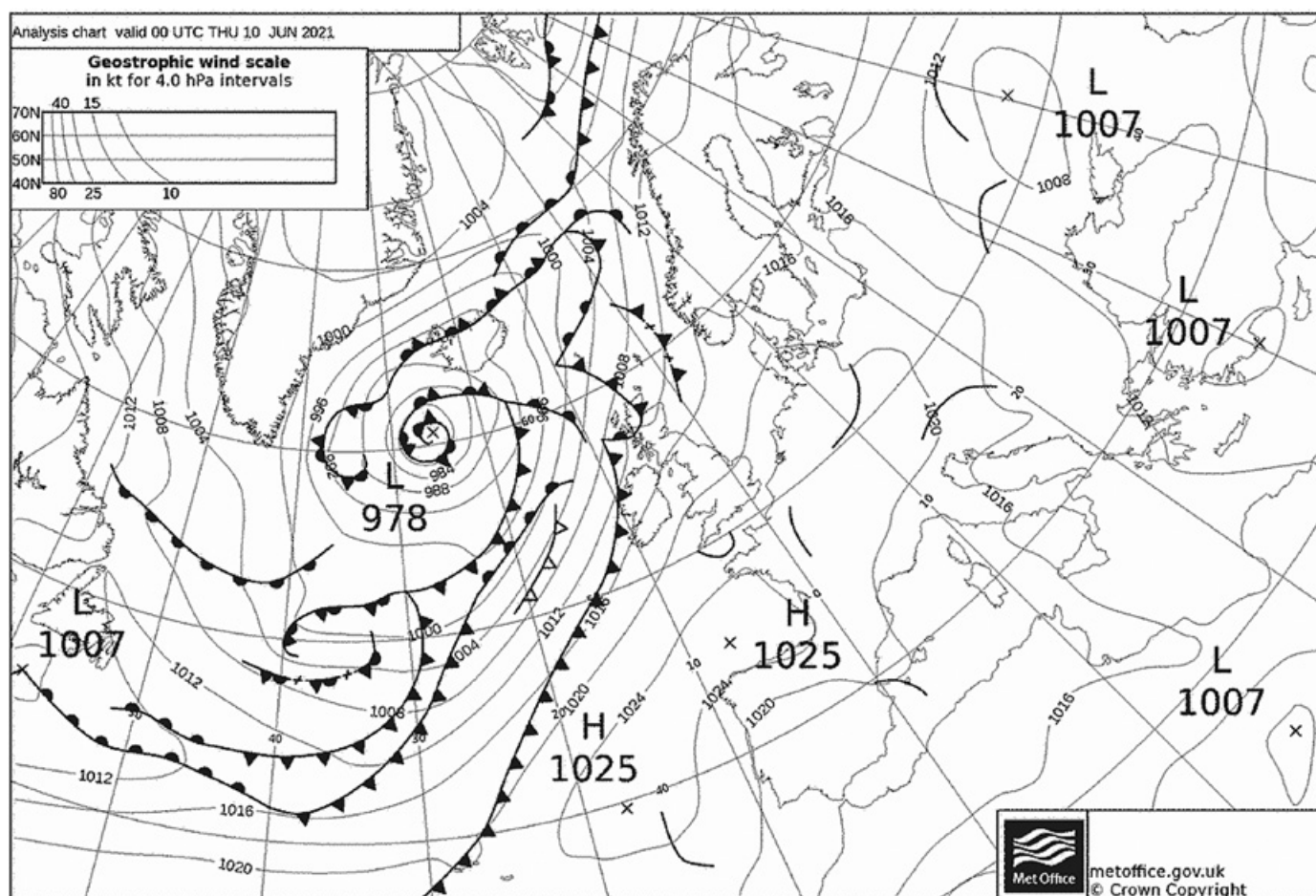eme east and northeast), it was early morning (between 0700 and 0900h local time), although the 24-hour Arctic summer daylight meant the Sun was still well above the horizon. The meteorological effects of this partial solar eclipse were expected to be discernible due to the season (near the summer solstice) and time of day when the Sun was at least several tens of degrees above the horizon as seen from most observation sites. Figures 2 and 3 provide a general perspective on weather conditions, especially cloud cover, during the eclipse period. A significant low pressure system with associated fronts and cloud affected much of the study region, although the south and east of the UK remained under the influence of a decaying anticyclone, albeit with a moist southwesterly airflow (Figure 2). All weather stations used in this study are from official networks or key baseline monitoring sites and captured high-time-frequency data

[2]Retrieved from the archive at https://www.wetterzentrale.de/

every 1 or 10min. This paper discusses the observations across the regions of interest, supplementing these with meteorological model results and also considers the effects on renewable energy generation.

British Isles

Data were acquired for 275 stations of the Met Office Meteorological Monitoring System (MMS), which record surface air temperature, relative humidity, mean sea-level pressure, wind speed and direction and cloud cover every minute, although a number of sites with incomplete records were not used in the analyses below. Solar radiation data were obtained for a partly overlapping network of 79 sites at 1-min time resolution. The sites used are listed in Tables S1 and S2 and their locations are shown in Figure S1 (Met Office, 2010) in the Supporting Information. A platinum resistance thermometer is used to measure near-surface (1.25 m height) air temperature to an accuracy of ±0.2degC, wind is typically measured using a traditional wind vane and cup anemometer (accuracy normally ±1 to 5%) and a LiDAR ceilometer measures cloud cover and height of the lowest cloud (i.e. cloud base) in a narrow column directly above the instrument every 30s (Met Office, 2010). The Met Office then use a sky condition algorithm to derive the total cloud cover based on a longer time series of data.

Based on the mean of 79 sites, solar (global) radiation initially peaked at ~350Wm⁻² around 0910–0920 UTC, then dropped back to ~281Wm⁻² at 1005–1010 UTC, a few minutes before the eclipse peak, before resuming its rise towards local noon, peaking at 473Wm⁻² at 1230 UTC (Figure 4). Averaging radiation data from four of the sites (Aberdaron, Almondsbury, Dundrennan and Eskdalemuir) that had constant total cloud cover or foggy conditions during the eclipse period shows that this dip in solar radiation coinciding with peak eclipse is robust (Figure 4) and unlikely to be a spurious effect arising from changes in cloud cover.

Total cloud cover estimated from ceilometer data for 107 sites, ranged between 7.2 and 7.5 oktas during the eclipse period. On average, cloud cover tended to increase slightly (by ~0.25 oktas) during the eclipse, although it decreased by ~0.1 oktas in the 15min prior to the eclipse peak (Figure 5). Only nine of the 107 sites (Aboyne, Albemarle, Bingley, Boulmer, Dyce, Fair Isle, Lossiemouth, Manston and Shoeburyness) had mean total cloud cover of <6 oktas between 0900 and 1130 UTC, with four stations (Albemarle, Boulmer, Manston and Shoeburyness) having mean cloud cover <4 oktas during this period. However, no site had clear skies (or nearly so) throughout the
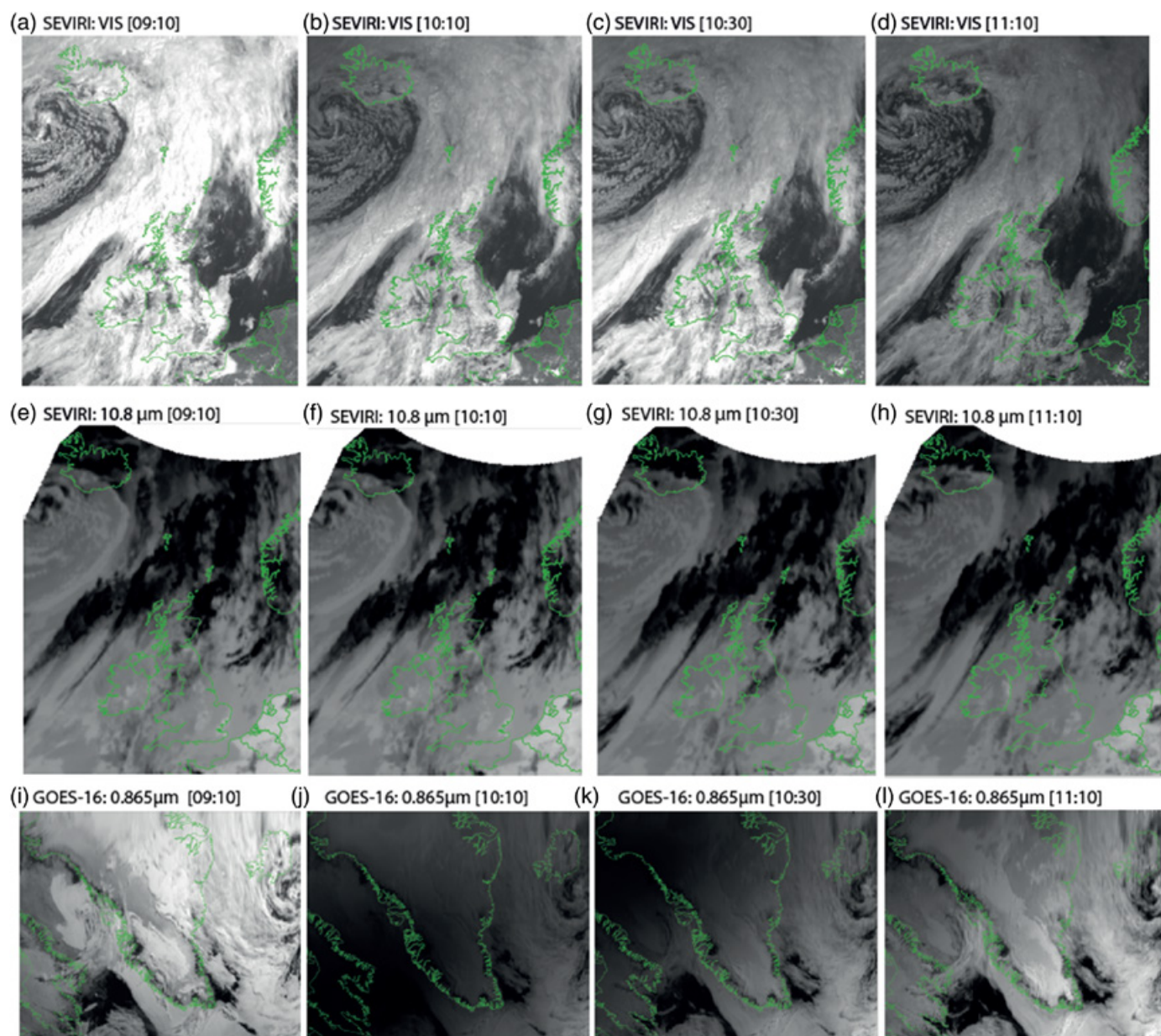
Figure 3. Satellite greyscale image sequences, showing cloud cover conditions during the eclipse period: (a–d) SEVIRI high-resolution visible broad bandwidth (0.6–0.9μm) images and (e–h) SEVIRI Ch9 thermal infrared, for the British Isles/Iceland; panels (i–l) show GOES 16 CM-03 (0.865μm) images of Greenland/Iceland. The eclipse shadow is evident in (j) and (k).

eclipse period. Also, all of the nine sites with relatively less cloud cover had significant changes in cloud cover during the eclipse, so were not a suitable subset to use for studying the eclipse influence on surface air temperature. Instead, we identified 14 sites with total and unchanging cloud cover or fog during 0900–1100 UTC as a more robust station subset for analysing temperature changes (see below).

Surface air temperature averaged from 254 MMS sites shows a marked reduction in the rate of increase of temperature around the time of peak eclipse (Figure 6a). The temperature initially rises quite sharply but then almost plateaus between 0930 and 1018 UTC before resuming its much steeper rise towards midday. Because this is a part of the day when temperature normally rises

quite steeply, it is appropriate to use regression analysis (which can be used to separate short-term deviations from a rising trend) to better isolate the effect of the eclipse on surface air temperature. We did this by removing mean temperature data between 0900 and 1130 UTC and, assuming a linear change in temperature, fitting a best-fit line to the data for the hour before and after this period (i.e. 0800–0900 UTC and 1130–1230 UTC; Figure 6b). We then took the difference or anomalies of the average 1-min temperature values with respect to the calculated regression line, which shows a temperature anomaly of −0.25 degC coinciding with the eclipse peak (Figure 6c). This is by far the largest temperature anomaly between 0800 and 1230 UTC. The relative temperature drop during the eclipse appears in 133 out of 255

individual MMS stations, although there is considerable scatter (Table S2). Repeating this regression analysis for the 14 sites with fixed and unchanging total cloud cover or foggy conditions during the eclipse also gave a similar result (Figure 6d). Also, the spatial pattern of the calculated temperature anomalies (Figure 7) shows the greatest negative effect along the eastern sides of England, parts of central and inland southwest England, northeast Scotland and parts of Northern Ireland (especially the northeast coast): these being regions where satellite imagery shows it was generally less cloudy during the eclipse (Figure 3). Eastern and northern coasts of the British Isles were relatively favoured in the prevailing moist southwesterly airflow (Figures 2 and 3). Therefore, we surmise that the relatively
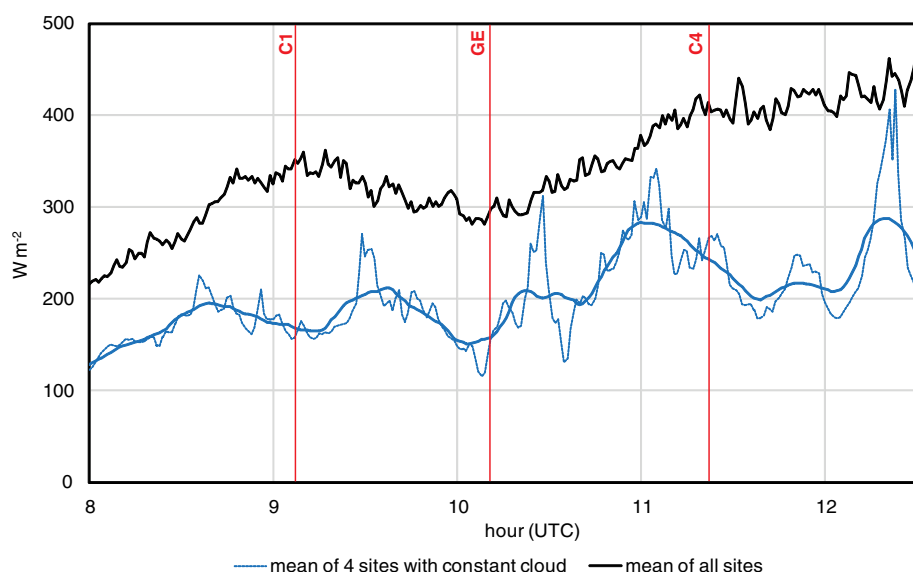
Figure 4. Global solar radiation from UK Met Office MMS weather stations on 10 June 2021: black line shows mean of 79 asterisked sites listed in Table S1, while the blue lines show the mean of four MMS sites (Aberdaron, Almondsbury, Dundrennan and Eskdalemuir) with known constant cloud/fog cover during 0900–1100 UTC (the bold blue line shows the 21-min running mean of the 1-min data). The vertical red lines marked C1, GE and C4 mark the beginning, peak and end of the eclipse.
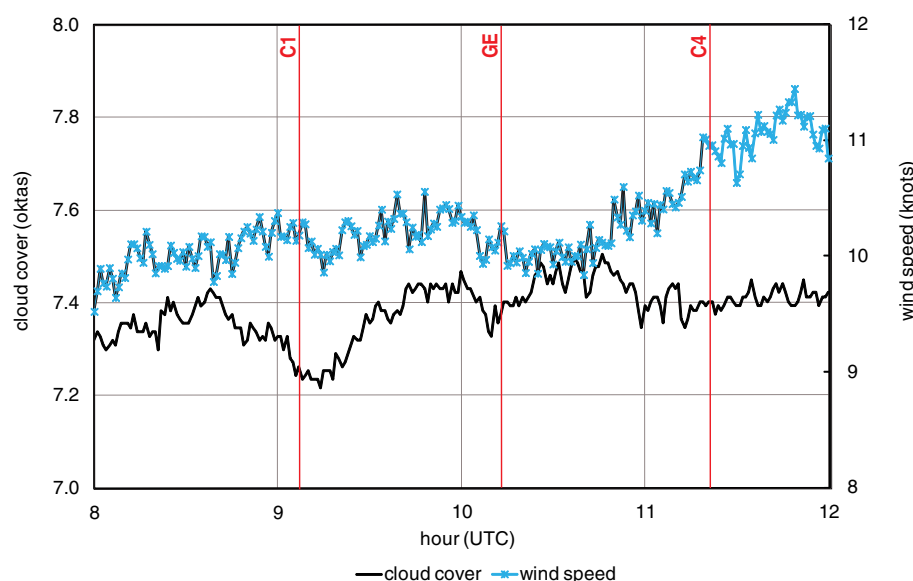

Figure 5. Mean total cloud cover and wind speed profiles for, respectively, 107 and 175 UK MMS weather stations on 10 June 2021. The beginning, peak and end of the eclipse are marked as in Figure 4.

low temperature anomaly centred around the eclipse peak but peaking 5–10min afterwards (as expected, due to thermal lag), although modest in magnitude, is not due to changes in cloud cover and is a robust feature due to the large number of stations analysed.

Finally, wind speed data averaged from MMS sites show a small dip ~10–15min after the eclipse peak (Figure 5). Since wind speed normally increases towards midday as part of the diurnal cycle, this is suggestive of an eclipse influence on the boundary layer but, due to the smaller change and greater short-term fluctuations in wind speed than temperature, is less persuasive than the temperature signal noted above.

Iceland

Conditions here too were generally cloudy during the eclipse (Table S3), but the eclipse magnitude was much larger than over the British Isles, being typically ~70% magnitude or ~60% coverage of the solar disk at peak eclipse (Figure 1). However, as in parts of the British Isles, the eclipse was seen either between clouds or through thin, high clouds. The station reporting the lowest cloud cover was in the northeast,

but there was little low cloud in parts of the west. Instantaneous 10-min temperature samples were available for 171 stations (Table S4; Figure S2). Most of these sites use a Logan platinum-resistance thermometer, most common type 4150, and all sites use a non-aspirated Young Multi-Plate Radiation Shield, with a quoted temperature accuracy of ±0.1 to 0.2 degC. Nearly all the stations use a Young anemometer. There is a very clear eclipse-related dip in the mean daily temperature profile from these sites, with instantaneous temperatures decreasing (in real terms) by 0.23 (±0.72) degC between 0910 and 1020 UTC, and by >0.6 degC in relative terms allowing for the diurnal temperature increase in mid-late morning (Figure 8). In addition, the maximum and minimum temperatures recorded every 10min were also available for many of these sites, so we were alternatively able to quantify the temperature decrease based on the highest temperature between 0830 and 0930 UTC (near the start of the eclipse) and the lowest temperature between 1000 and 1100 UTC (around the eclipse peak). This alternative method identified a larger cooling, partly because of short-term fluctuations in temperature, with a somewhat larger mean 1.08 (±0.77) degC temperature dip coinciding with the eclipse. The plus/minus values refer to the standard deviation of all the station values used in the respective mean temperature. Given short-term fluctuations in wind speed, there is little sign of an eclipse-related influence on wind (Figure 8). There is no significant relation between mean wind speed during the eclipse (0900–1130 UTC) and temperature reduction at the same time.

Greenland

Again, ambient conditions were mainly cloudy. As with Iceland, Greenland meteorological data were acquired every 10min for all sites except Summit, which logged data every minute (Table S5). Seven coastal Greenland stations of the Danish Meteorological Institute (DMI) synoptic network in Greenland (Cappelen, 2021; Table S5 and Figure S3) have 10-min data and so were used. DMI stations use a Vaisala temperature sensor (accuracy ~±0.25 degC) housed in a naturally-ventilated RM Young Multi-Plate Radiation Shield. These sites show an average 0.2 or 0.6 degC actual reduction in temperature (using the same two measures as for Iceland) centred on the eclipse (Table 1, Figure 9a); this appears as a dip in the diurnal temperature profile that averages data from all these stations (Figure 9b). Temperature drops (defined for these sites as 1020 minus 0910 UTC temperature) ranged from 0.1 degC at 04272 Qaqortoq to 0.8 degC at 04320 Danmarkshavn and 04339 Ittoqqortoormiit. However, 04360 Tasiilaq on the east coast

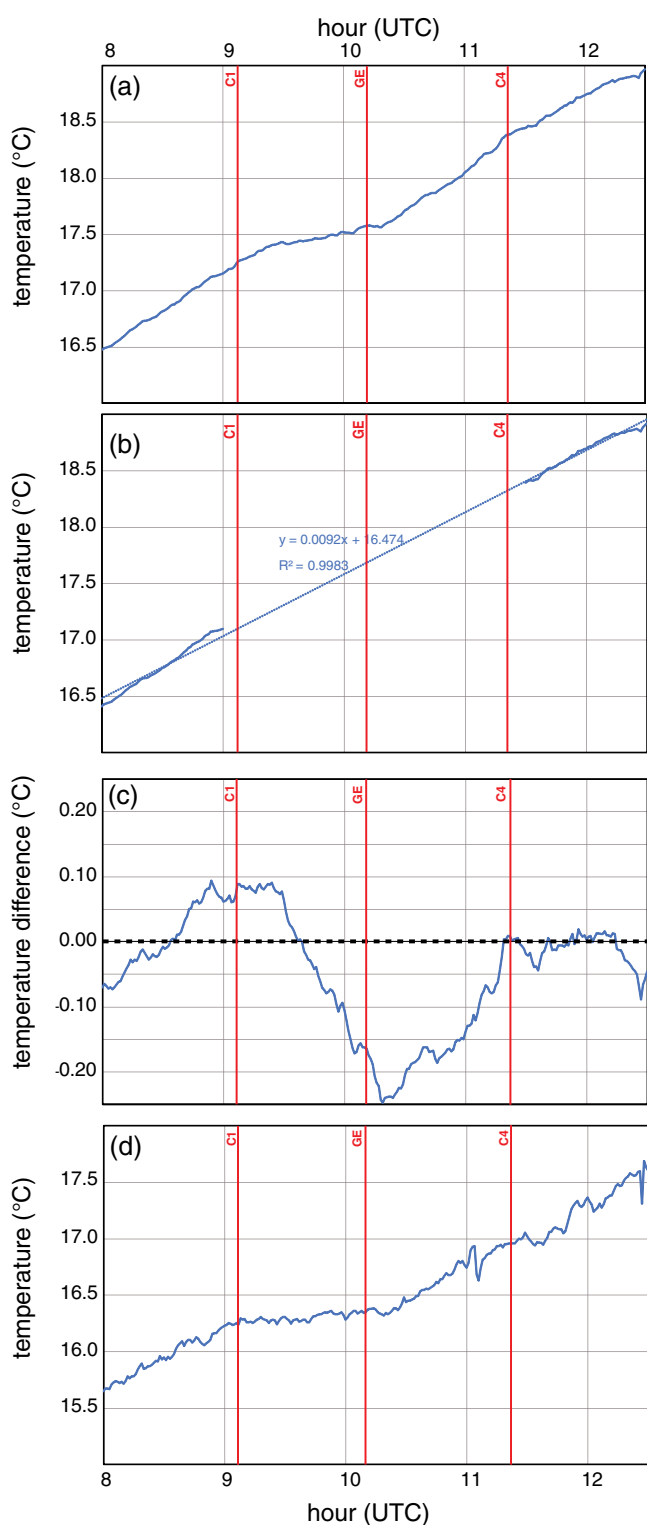**RMetS**
Royal Meteorological Society

Figure 6. Mean surface air temperature profile for 10 June 2021: (a) based on 254 UK Met Office MMS automatic weather stations; (b) with central data removed and regression line fitted through; (c) temperature anomalies with respect to the calculated regression line and (d) mean temperature profile of 14 MMS sites with constant cloud/fog cover during 0900–1100 UTC. See main text for details. The beginning, peak and end of the eclipse are marked as in Figure 4.

was greatest. Reasons for this may include cloud cover which dominated at the time of eclipse (Figure 3) as well as a possible moderating influence of the ocean and/or downslope katabatic winds on temperature changes at these mainly coastal sites, which are peripheral to a giant ice sheet.

Next, we analysed data from five automatic weather stations from the Programme for monitoring of the Greenland Ice Sheet (PROMICE) covering the Greenland Ice Sheet interior, run by the Geological Survey of Denmark and Greenland (GEUS) (Fausto *et al.*, 2021; Table S5 and Figure S3). The PROMICE data include percentage cloud cover estimated from downward longwave radiation and air temperature from an actively ventilated PT100 probe (accuracy ± 0.1 degC). The PROMICE stations show larger mean temperature decreases of about 0.4 or 1.3 degC and similar wind speed reductions, relative to the coastal Greenland DMI stations, during the eclipse (Table 1; Figures 11 and S5). For completeness, we also show corrected downward shortwave radiation and estimated cloud cover profiles for the PROMICE sites (Figures S6 and S7). Downward shortwave radiation averaged across these sites reduced during the eclipse from 291.1Wm^{-2} at 0930 UTC to 83.4Wm^{-2} at 1030 UTC, with the largest reduction of 88.5% at THU_L in northwest Greenland, which experienced the greatest eclipse magnitude. Mean estimated cloud cover during 0900–1130 UTC was 15.1 (± 8.0)% at CEN, 68.1 (± 20.6)% at EGP, 14.3 (± 2.6)% at KAN_L, 70.5 (± 19.8)% at KAN_M and 2.8 (± 2.3)% at THU_L (where the plus/minus values indicate one standard deviation of the variation of the 10-min values). Therefore, out of the five PROMICE sites, THU_L had the clearest conditions and most stable (small) cloud cover during the eclipse. Cloud cover at these interior Greenland sites tended to decrease during the eclipse, although there was considerable spatial and temporal variability (Table 1; Figure S7).

Finally, we examine 1-min data from NOAA's GEOSummit station[3] located in the centre and on top of the Greenland Ice Sheet at 3210m above sea level (Figure S3/Table S5). During the eclipse, Summit showed a temperature reduction of 0.3 and 2.9 degC (according to definition; Table 1), but no clear change in wind speed (Table 1; Figure 12).

Regional climate model eclipse simulation

Figure 13 shows the effect of the eclipse on mean downward shortwave radiation, 2m temperature and 10m wind, based on two simulations with and without the eclipse for the period 0930 to 1130 UTC (2-hour mean) on 10 June 2021 run using the MAR regional

of Greenland was the exception in showing a 1.3 degC temperature increase over this period, which this may have been due to changes in local weather conditions masking the effect of the eclipse. There is a pronounced dip in mean solar (global) radiation at six sites from ~250Wm^{-2} at 0910 UTC to <90Wm^{-2} at 1030 UTC (Figure 10).

Wind speed was also relatively low around the time of the eclipse, with a mean reduction of about 30% according to the metric used (Table 1), although there was substantial short-term variability (Figure S4). The reduction in temperature is relatively modest compared with what might have been expected for this region where the eclipse

---

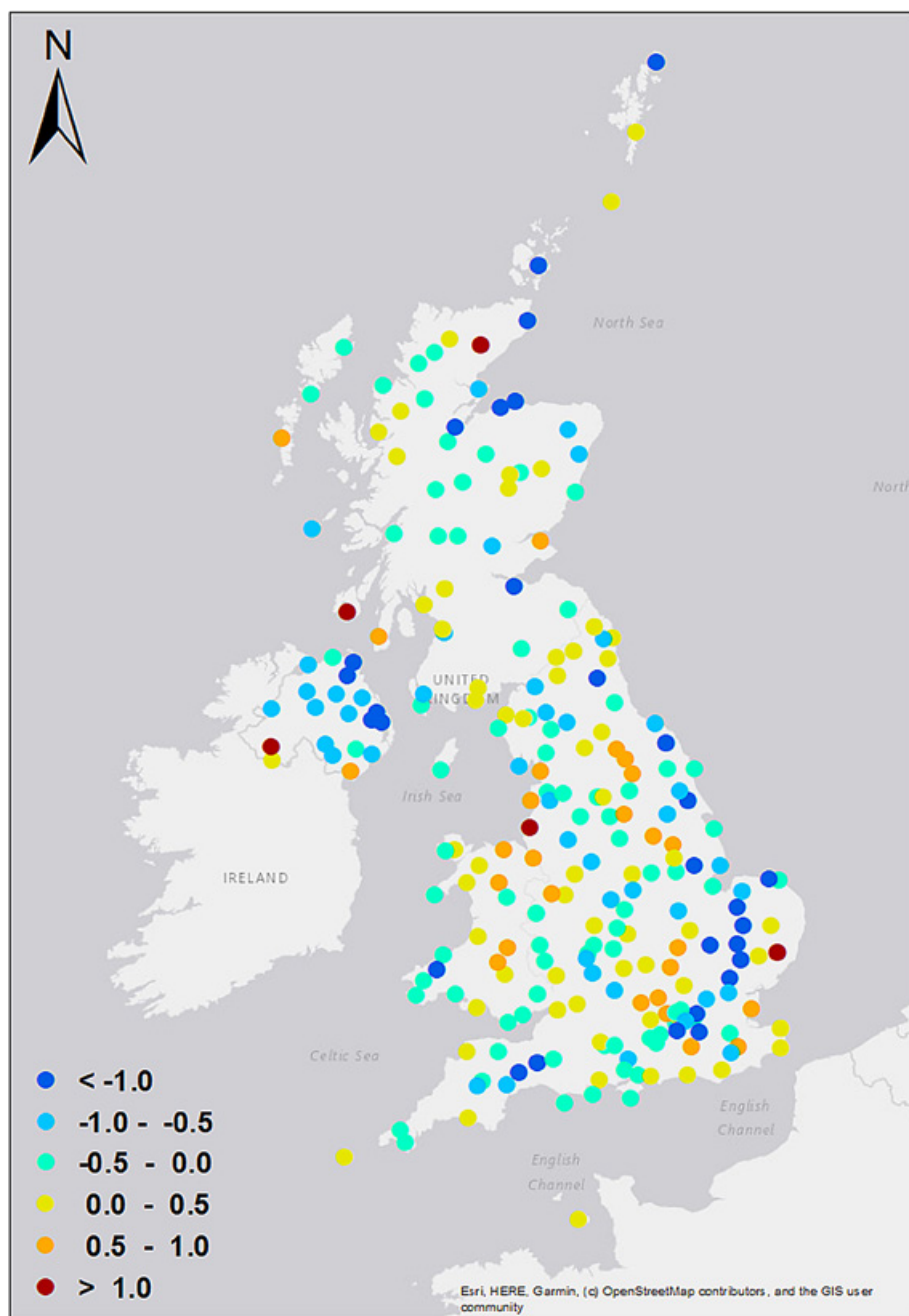[3]http://geo-summit.org/summit-station

Figure 7. Temperature anomalies (degC) across the British Isles at 1019 UTC on 10 June 2021 (a few minutes after the peak of the eclipse), calculated using the regression-based method described in the main text. Negative values indicate local temperatures trending lower around the time of mid-eclipse.

climate model (Fettweis *et al*., 2020) at a resolution of 20km. MAR was forced every 6 hours at its lateral boundaries by temperature, wind and specific humidity data from the European Centre for Medium Range Weather Forecasts (ECMWF) ERA5 reanalysis (Hersbach *et al*., 2020). The solar constant was reduced in the MAR radiative scheme (Fettweis *et al*., 2021) to take the effect of the eclipse into account, with a correction varying in space and time according to Figure 1. This methodology has previously been used to simulate meteorological effects of previous eclipses (Gray and Harrison, 2012) but is extended here to consider eclipse effects on the Greenland Ice Sheet.

MAR is widely used in Greenland climate and ice-sheet surface mass balance studies (e.g. Fettweis *et al*., 2020; Hanna *et al*., 2021) and has also been used in additional studies across the wider domain shown in Figure 13 (Wyard *et al*., 2017, 2018). Radiation differences largely reflect variations in cloud cover (Figure 3) but are often largest across land areas (Figure 13a). The greatest shortwave radiation differences of up to 270Wm^{-2} are unsurprisingly located in Greenland (where the eclipse was greatest) where they are focused in central and northern parts of the island, with a maximum around and just to the south/southeast of Summit. Iceland shows relatively modest reductions

in downward shortwave radiation, which is likely to be a function of largely cloudy conditions there (Figure 3; Table S3). The British Isles have low to moderate reductions in downward shortwave radiation, with the greatest response in the extreme east of England, the Welsh borders running up to Merseyside, eastern and northern Scotland and some northern and eastern parts of Ireland (Figure 13a) – largely the same areas with the greatest eclipse-related temperature reductions.

MAR-simulated surface air temperature differences with and without the eclipse generally reflect solar radiation differences: the greatest 2-hour mean temperature differences of −1 to −2 degC are seen in interior central and northwest Greenland but with isolated small spots of similar magnitude in interior Iceland and slightly bigger such areas in parts of northeast and central England and northeast Scotland (Figure 13b). Average whole-country temperature differences around the peak of the eclipse were −1.3 degC (Greenland), −0.3 degC (Iceland) and −0.6 degC (UK). The surface wind field from MAR shows little change over the British Isles, except for a slight reduction of 0.5–1.0ms^{-1} along the northeast Scotland coast, a few isolated spots of slightly (~1.0ms^{-1}) reduced wind in interior/southern Iceland, but significant areas of katabatic wind field change over the Greenland Ice Sheet (Figure 13c). These latter include reduced winds during the eclipse in the central and eastern Greenland interior to the north and south of Summit but increased winds in the west and northwest and along the southeast coast, linked with circulation anomalies in the katabatic winds, focused in central eastern, central northern and southern Greenland. We note there appears to be less change at Summit itself, in line with the observational data reported above (Figure 12). Finally, from MAR, we show the impact of the eclipse on the amount of surface meltwater generated over the Greenland Ice Sheet (Figure 14). The eclipse delays ice-sheet melt onset by a few hours, which results in 9% less surface melt at the end of the day in the model simulation with the eclipse compared with the control run.

Effect of the eclipse on UK renewable energy production

Solar eclipses have a direct effect on renewable electricity generation, through the reduction in both photovoltaic (PV) generation and wind speed. Monitoring systems for electricity generation can therefore also be used indirectly to provide a wide-area average of the eclipse effects, as in the UK during the 2015 eclipse (Harrison and Gray, 2017), or alternatively, to evaluate weather effects on energy generation.

Figure 15 presents an analysis of the different effects in these two renewable sources of energy. In all four panels, the relative variation in top of atmosphere solar radiation on a horizontal surface on 21 June has been calculated for Birmingham (gold line), following the method of Harrison *et al.* (2016). In (a), variations in solar generation in northern Scotland, northeast England and southern England are shown. There is little response to the eclipse in southern England, but the other two regions show a dip in the load factor (the proportion of the total generation) coincident with the eclipse timing. In (b), the national PV generation is shown, which essentially averages across all the sites, reducing the variability. This shows a clear signal at the eclipse time, with a flattening out and slight drop in the power generation curve at maximum eclipse time, a time of day when the PV output would normally be increasing strongly. (This drop exceeds −1.5 standard deviations of the normal expected for this time of day in June, based on 30-min values calculated over the period 2013–2020.) Immediately after the eclipse, the solar PV curve recovers quickly, as expected, to normal values, but it also exhibits an interesting 'overshoot' at 1200 UTC where it surpasses the mean PV by some ~7%, before returning to slightly below the mean by 1300 UTC. This is probably a cloud effect, involving some dissipation of low cloud (probably convective cumulus and stratocumulus) during the eclipse due to reduced solar radiation, which ceased within an hour or so after the end of the eclipse. Reductions in cloud cover, especially low cloud (which are optically thickest), have been noted in previous eclipses (e.g.
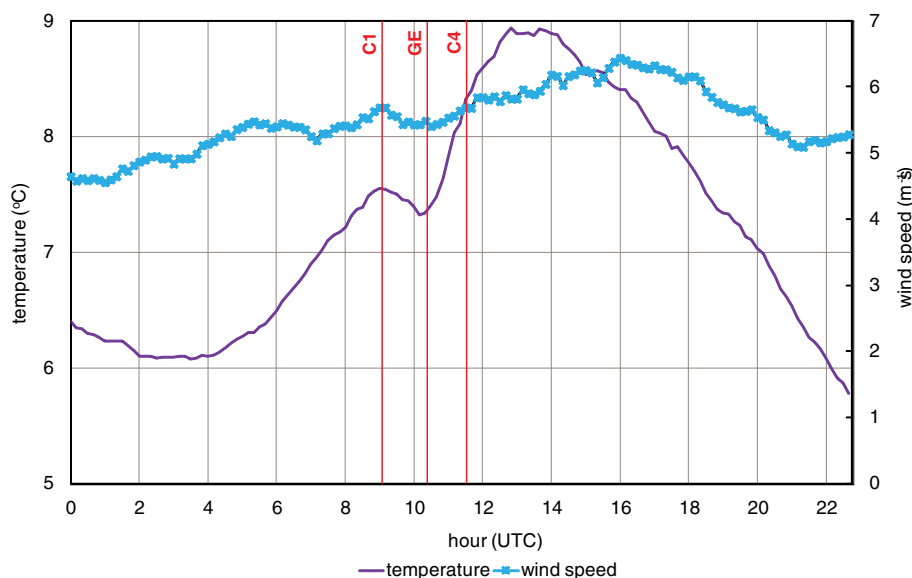

Figure 8. Icelandic weather stations mean surface air temperature profile based on 170 sites and wind speed profile based on 255 sites for 10 June 2021. The beginning, peak and end of the eclipse are marked as in Figure 4.

Table 1

Change in temperature (degC), wind-speed (ms⁻¹) and (where available) estimated cloud cover (%) Greenland weather stations during the 10 June 2021 eclipse. For PROMICE sites, we use the mean of the two temperature sensors (except for Kan-L where the secondary sensor did not return data)

Station	1020 minus 0910 temperature (degC)	Lowest temperature during 1000–1100 minus highest temperature during 0830–0930	1020 minus 0910 wind speed (ms⁻¹) with equivalent percentage change	Lowest wind speed during 1000–1100 minus highest wind speed during 0830–0930	1020 minus 0910 estimated cloud cover (Lowest cloud cover during 1000–1100 minus highest cloud cover during 0830–0930)
DMI sites					
04220	−0.3	−0.3	−0.5 (−17%)	−1.6 (−42%)	N/A
04250	−0.2	−0.4	−0.3 (−8%)	−2.4 (−52%)	N/A
04271	−0.5	−0.9	+1.4 (N/A)	0.0 (0%)	N/A
04272	−0.1 (est.)	−0.3	N/A	N/A	N/A
04320	−0.8	−1.0	−3.1 (−53%)	−3.6 (−60%)	N/A
04339	−0.8	−1.0	−0.1 (−1%)	−1.9 (−19%)	N/A
04360	+1.3	−0.5	0.0 (0%)	−0.5 (−100%)	N/A
DMI mean	**−0.20**	**−0.63**	**−0.43 (−16%)**	**−1.67 (−46%)**	**N/A**
PROMICE sites					
CEN	−0.77	−1.39	−1.00 (−26%)	−3.01 (−66%)	−19% (−45%)
EGP	−0.78	−2.06	−1.43 (−63%)	−2.20 (−72%)	−38% (−65%)
Kan L	−0.19	−0.59	+2.21 (+3683%)	−0.06 (−3%)	−3% (−7%)
Kan M	−0.21	−0.50	+0.02 (+0.1%)	−0.62 (−20%)	+53%(−13%)
Thule L	−0.09	−1.85	−2.08 (−14%)	−5.23 (−33%)	−3% (−7%)
PROMICE mean	**−0.41**	**−1.28**	**−0.46 (+716%)**	**−2.22 (−39%)**	**−2% (−27%)**
Summit	−0.30	−2.90	+0.60 (+14%)	−1.40 (−32%)	N/A

All times are UTC.

DMI, Danish Meteorological Institute; PROMICE, Programme for monitoring of the Greenland Ice Sheet.
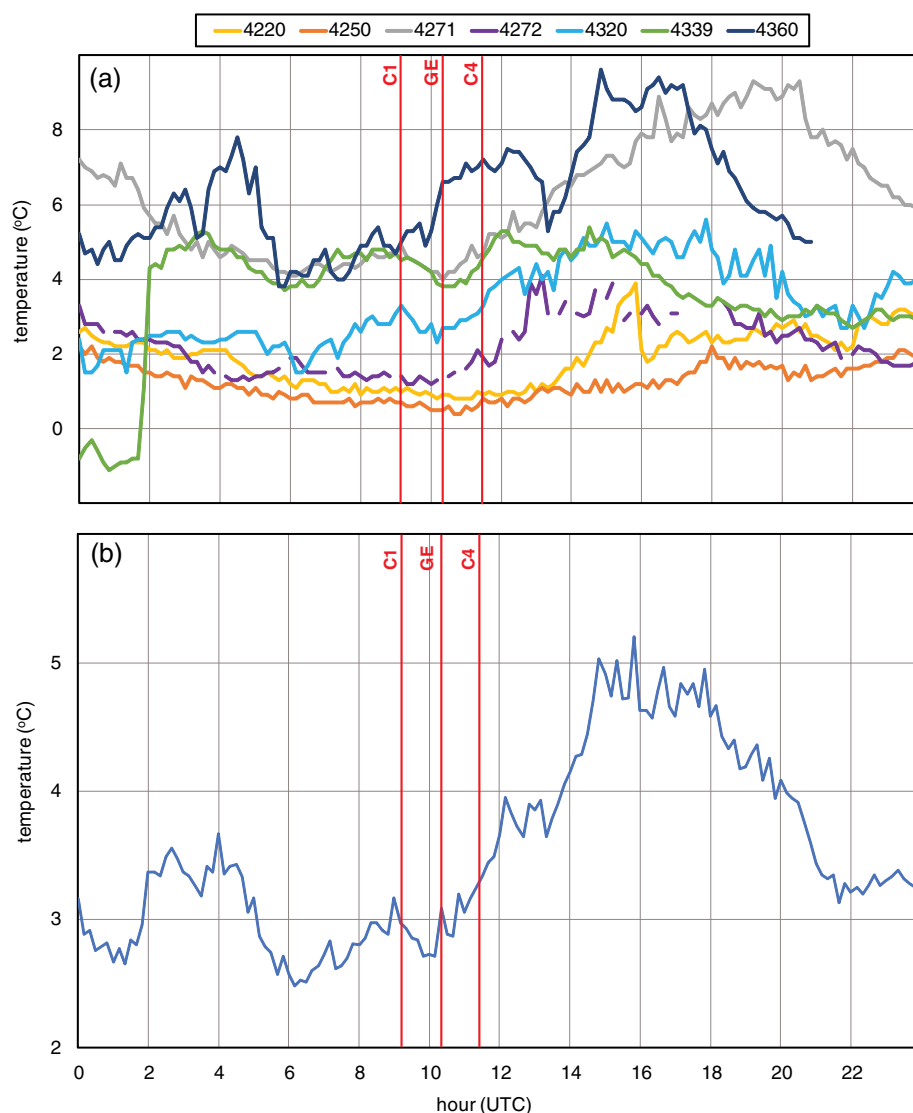
Figure 9. Surface air temperature profiles for 10 June 2021 for (a) seven Danish Meteorological Institute (DMI) coastal Greenland weather stations and (b) the mean profile. The beginning, peak and end of the eclipse are marked as in Figure 4.

Hanna, 2000), and the timeframe of the solar PV recovery lies well within what might be expected meteorologically during daytime in June.

Figure 15(c) and (d) consider the effect on wind generation, using data from multiple small wind turbines. In (c), the data from the multiple sites are not intended to be specifically identified and are plotted in 'spaghetti' form to illustrate the variability between different sites in which no consistent signal is apparent at the eclipse time (see also Figure 5). If these are averaged together, however, a small effect following the minimum in solar radiation becomes evident. Further examination of the individual sites revealed the strongest effect in the East Midlands, which is shown in (d). Despite the relatively coarse time resolution of the data (hourly), the minimum in the wind generation occurs later than the minimum in solar radiation. This effect in the East Midlands (d) is consistent with a 22% decrease in the running mean wind speed of the 11 Met Office MMS sites in the East Midlands compared with

a mean 4% decrease in the running mean wind speed nationally across all the UK MMS sites. A displaced wind speed minimum of about 30min after the solar radiation minimum also occurred in observations from the 2015 eclipse, using 1-min data (Gray and Harrison, 2016). A related delay in the UK wind-driven electricity generation was also apparent (Harrison and Gray, 2017), supporting a possibly consistent feature of wind electricity generation during eclipses.

Discussion and summary

Prevailing air masses on 10 June 2021 gave generally cloudy conditions over the region of interest, but local cloud variations resulted in clear differences in the meteorological signature and impacts of the eclipse at the local to regional level. Temperature decreases of about 0.5–2 degC were seen for the Iceland and Greenland sites, with relatively smaller temperature drops observed in the British Isles (~0.25 degC): values that

are unsurprisingly relatively small compared with many studies of total solar eclipses but which are nevertheless robust based on the large number of stations analysed here, having controlled (where possible) for changes in cloud cover. We also provide evidence of systematic decreases in wind speed during the eclipse, despite ambient cloud cover. Some changes noted are not large but are nevertheless quite clear due to the large number of weather station time series analysed. The observed eclipse signature is well borne out through regional climate model simulations. The model runs confirm the greatest response over Greenland as well as a significant reduction in daily-integrated ice melt on 10 June 2021 due to the eclipse. Also, there were discernible reductions at local and national scale of solar and wind renewable energy production in the UK. As for the 2015 eclipse, the reduction in wind generation was observed to occur after the reduction in solar PV generation, prolonging the total impact on renewable energy generation. This is likely to be associated with the slow thermal response of the surface to the restoration of solar heating, delaying the return of convectively-driven wind.

Continued expansion in renewable energy systems globally is likely to lead to more transient solar eclipse effects on electrical power generation. A primary aspect which emerges for eclipse energy planning is that expected reductions in solar generation of electricity cannot be reliably mitigated through wind generation alone, as this alternative renewable source of energy is also affected by a solar eclipse. Forecasting the impact of an eclipse on the energy generation, which is necessary for stable energy supply planning, will therefore require accurate regional weather forecasts, to predict both the solar PV and wind generation reductions and their timings. Knowledge of the solar radiation reduction alone using the astronomical circumstances is likely to be insufficient, as the effect of cloud (as observed here) is also critical to the solar PV generation. The timing of the recovery of the wind generation may also be highly relevant. Numerical models for weather forecasting, which include the effects of an eclipse (e.g. Clark, 2016), may therefore need to be further developed for the energy sector.

We hope our findings demonstrate the value of studying the meteorological effects and wider impacts of partial solar eclipses. Cloud primarily controls the surface temperature response, yet it can be difficult to obtain consistent surface data on cloud variations. This supports the use of citizen science to acquire more detailed information on local cloud changes for future eclipses, supplementing the relatively limited surface observations and broad-scale satellite imagery (Barnard *et al.*, 2016). More comprehensive meteorological data acquired from a wider range of solar eclipses, and associated
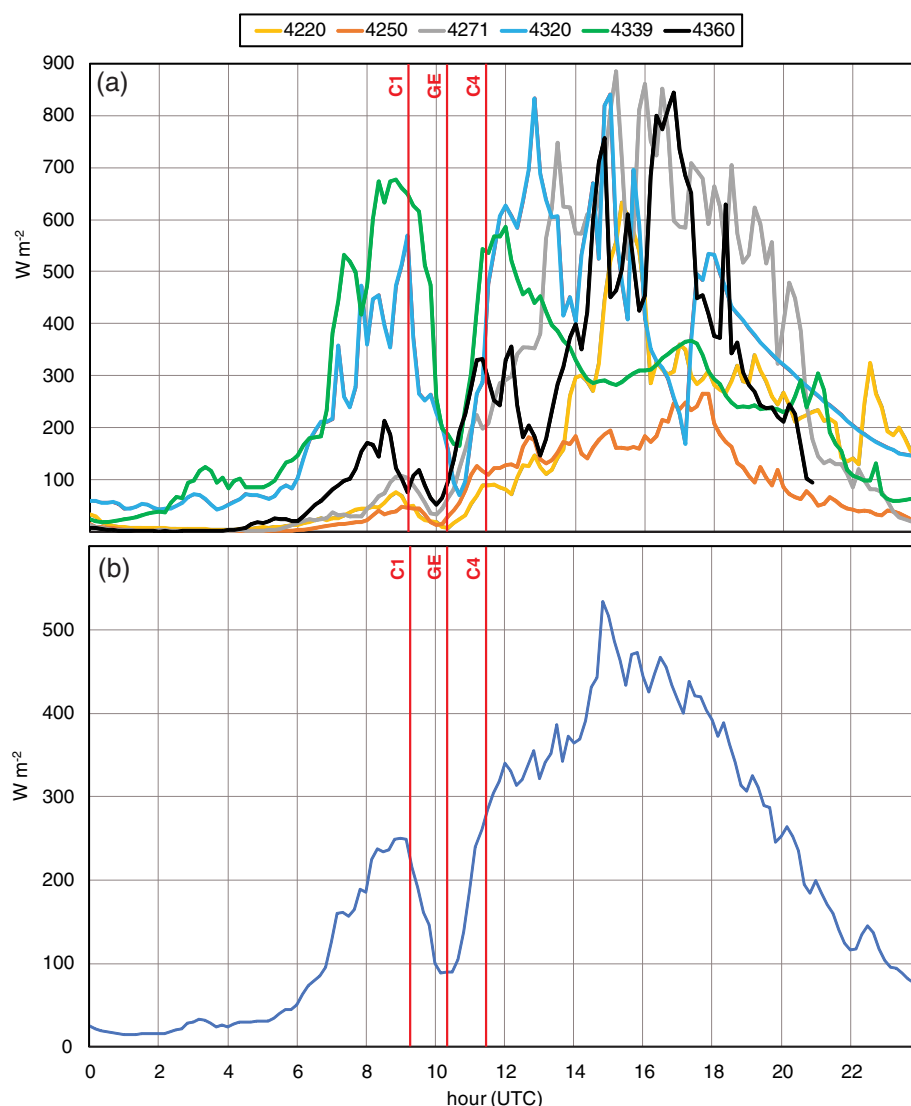
Figure 10. Global solar radiation profiles for 10 June 2021 for (a) seven DMI coastal Greenland weather stations and (b) the mean profile. The beginning, peak and end of the eclipse are marked as in Figure 4.

modelling of the key energy input into the atmosphere, also have the potential to improve our understanding of atmospheric response to climate change.

Acknowledgements

References

Aplin KL, **Harrison RG**. 2003. Meteorological effects of the eclipse of 11 August 1999 in cloudy and clear conditions. *Proc. R. Soc. A* **459**(2030): 353–371.

Aplin KL, **Scott CJ**, **Gray SL**. 2016. Atmospheric changes from solar eclipses. *Phil. Trans. R. Soc. A* **374**: 2015.0217.

Barnard L, **Portas AM**, **Gray SL** *et al*. 2016. The National Eclipse Weather Experiment: an assessment of citizen scientist weather observations. *Phil. Trans. R. Soc. A* **374**: 2015.0220.

Cappelen J. 2021. Weather observations from Greenland 1958-2000. DMI Report No. 21-08, Danish Meteorological Institute: Copenhagen. https://www.dmi.dk/fileadmin/Rapporter/2021/DMIRep21-09.pdf [accessed 21 February 2022].

Clark PA. 2016. Numerical simulations of the impact of the 20 March 2015 eclipse on UK weather. *Phil. Trans. R. Soc. A* **374**: 2077

Fausto RS, **van As D**, **Mankoff KD** *et al*. 2021. Programme for Monitoring of the Greenland Ice Sheet (PROMICE) automatic weather station data. *Earth Syst. Sci. Data* **13**: 3819–3845.

Fettweis X, **Hofer S**, **Krebs-Kanzow U** *et al*. 2020. GrSMBMIP: intercomparison of the modelled 1980–2012 surface mass balance over the Greenland Ice Sheet. *Cryosphere* **14**: 3935–3958.

Fettweis X, **Hofer S**, **Séférian R** *et al*. 2021. Brief communication: Reduction in the future Greenland ice sheet surface melt with the help of solar geoengineering. *Cryosphere* **15**: 3013–3019.

Gray SL, **Harrison RG**. 2012. Diagnosing eclipse-induced wind changes. *Proc. R. Soc. A* **468**(2143): 1839–1850.

Gray SL, **Harrison RG**. 2016. Eclipse-induced wind changes over the British Isles on the 20 March 2015. *Phil. Trans. R. Soc. A* **374**: 2015.0224.

Hanna E. 2000. Meteorological effects of the solar eclipse of 11 August 1999. *Weather* **55**: 430–446.

Hanna E. 2018. Meteorological effects of the 20 March 2015 solar eclipse over the United Kingdom. *Weather* **73**: 71–80.

Hanna E, **Penman J**, **Jónsson T** *et al*. 2016. Meteorological effects of the solar eclipse of 20 March 2015: analysis of UK Met Office automatic weather station data and comparison with automatic weather station data from the Faroes and Iceland. *Phil. Trans. R. Soc. A* **374**: 2015.0212.

Hanna E, **Cappelen J**, **Fettweis X** *et al*. 2021. Greenland surface air temperature changes from 1981 to 2019 and implications for ice-sheet melt and mass-balance change. *Int. J. Climatol.* **41**: E1336–E1352.

Harrison RG, **Gray SL**. 2017. The weather's response to a solar eclipse. *Astron. Geophys.* **58**: 4.11–4.16.

Harrison RG, **Hanna E**. 2016. Atmospheric effects of solar eclipses stimulated by the 2015 UK eclipse. *Phil. Trans. R. Soc. A* **374**: 2015.0217.

Harrison RG, **Marlton GJ**, **Williams PD** *et al*. 2016. Coordinated weather balloon solar radiation measurements during a solar eclipse. *Phil. Trans. R. Soc. A* **374**: 2015.0221.

Hersbach H, **Bell B**, **Berrisford P** *et al*. 2020. The ERA5 global reanalysis. *Q. J. R. Meteorol. Soc.* **146**: 1999–2049.

Met Office. 2010. National Meteorological Library and Archive Fact Sheet 17 – Weather observations over land. https://www.metoffice.gov.uk/binaries/content/assets/metofficegovuk/pdf/research/library-andarchive/library/publications/factsheets/factsheet_17-observationsv02.pdf.

Wyard C, **Scholzen C**, **Fettweis X** *et al*. 2017. Decrease in climatic conditions favouring floods in the south-east of Belgium over 1959–2010 using the regional climate model MAR. *Int. J. Climatol.* **37**: 2782–2796.

Wyard C, **Doutreloup S**, **Belleflamme A** *et al*. 2018. Global Radiative Flux and Cloudiness Variability for the Period 1959–2010 in Belgium (2018) A Comparison between Reanalyses and the Regional Climate Model MAR. *Atmosphere* **9**: 262.

Supporting Information

Table S1. Details of UK Met Office MMS weather stations used in this study. Solar radiation data were available/used from a subset of 79 sites marked with an asterisk.

RMetS
Royal Meteorological Society

Table S2. Magnitude of surface air temperature dip (negative anomaly relative to least squares trend line fit, as described in the main text) and its timing at individual UK Met Office MMS weather stations during 0900 to 1130 UTC on 10 June 2021. Where the 1-min temperature did not dip below the regression line and/or where there is no clear signal corresponding with the eclipse period, this is indicated as 'N/A'. The relative temperature anomaly at 1019 UTC (a few minutes after the eclipse peak) is also shown, and is shaded in green (yellow) for stations where there is a clear signal of at least −1.0 (−0.5) degC and in grey where there is a smaller negative temperature anomaly.

Table S3. Cloud cover conditions during the 10 June 2021 eclipse period for available weather stations in Iceland. Low, medium and high cloud types follow World Meteorological Organization classifications (https://cloudatlas.wmo.int/en/cloud-classification-aids-cl-cm-ch.html). Data courtesy of the Icelandic Met Office (IMO).

Table S4. Details of 171 Icelandic Met Office weather stations with surface air temperature records used in this study.

Table S5. Details of Greenland weather stations used in this study. DMI station metadata are from Cappelen (2021). Summit data are from https://gml.noaa.gov/dv/site/site.php?code=SUM

Figure S1. Map showing UK Met Office MMS weather stations used in this study (note the map also shows a few additional stations not used here). For cross-reference with station details, please see Table S1.

Figure S2. Map showing the 171 Icelandic weather stations with surface air temperature data used in this study.

Figure S3. Map showing Greenland weather stations used in this study. Station details are provided in Table S5.

Figure S4. Wind-speed profiles for 10 June 2021 for seven DMI coastal Greenland weather stations (a) and the mean profile (b).

Figure S5. Wind speed profiles for 10 June 2021 for five PROMICE Greenland Ice Sheet weather stations (a) and the mean profile (b).

Figure S6. Corrected downward shortwave radiation profiles for 10 June 2021 for five PROMICE Greenland Ice Sheet weather stations (a) and the mean profile (b).

Figure S7. Estimated cloud cover profiles for 10 June 2021 for five PROMICE Greenland Ice Sheet weather stations (a) and the mean profile (b).

Correspondence to: E. Hanna
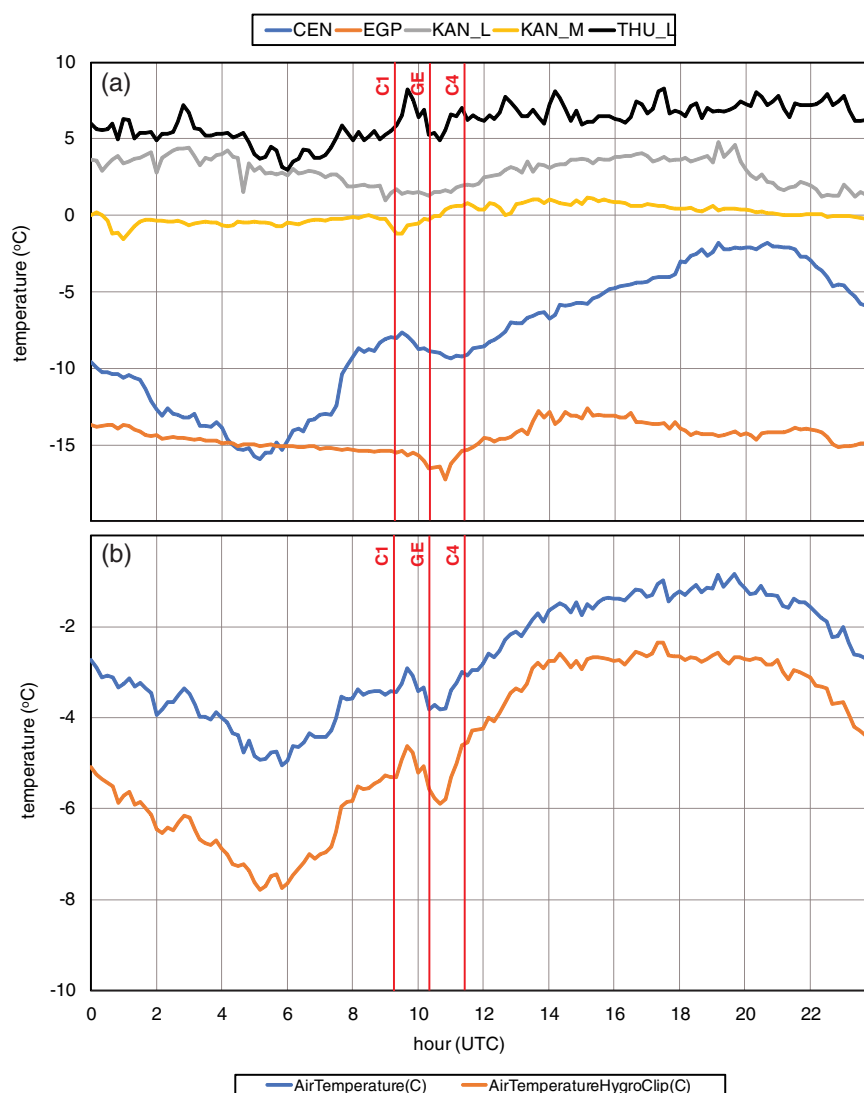
ehanna@lincoln.ac.uk

Figure 11. Surface air temperature profiles for 10 June 2021 for (a) five PROMICE Greenland Ice Sheet weather stations and (b) the mean profile (blue line) and that from auxiliary thermometers (orange line). The beginning, peak and end of the eclipse are marked as in Figure 4.
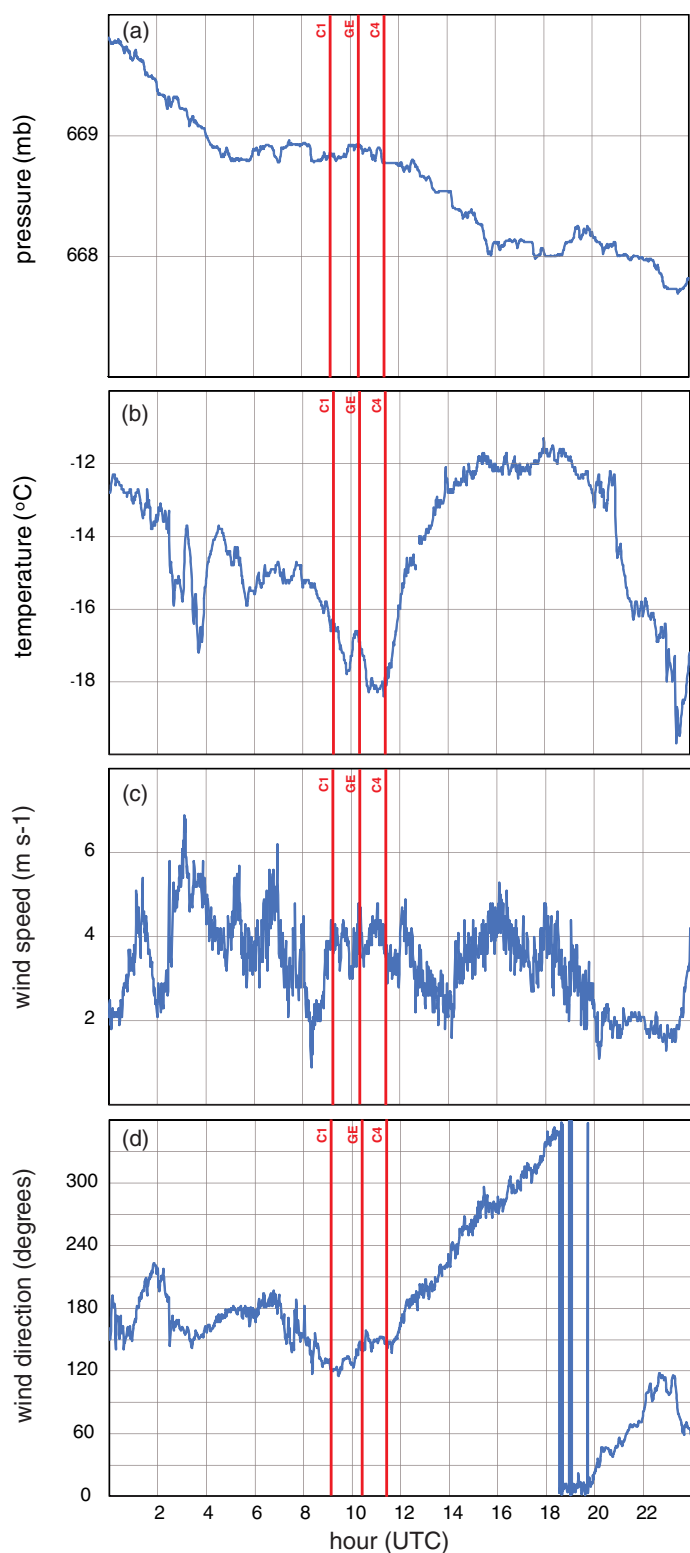
Figure 12. Summit, Greenland, meteorological parameters on 10 June 2021: (a) barometric pressure; (b) surface air temperature; (c) wind speed and (d) wind direction. The beginning, peak and end of the eclipse are marked as in Figure 4.

(a) Mean difference in shortwave radiation (w/m²)

(b) Mean difference in 2m–temperature (°C)
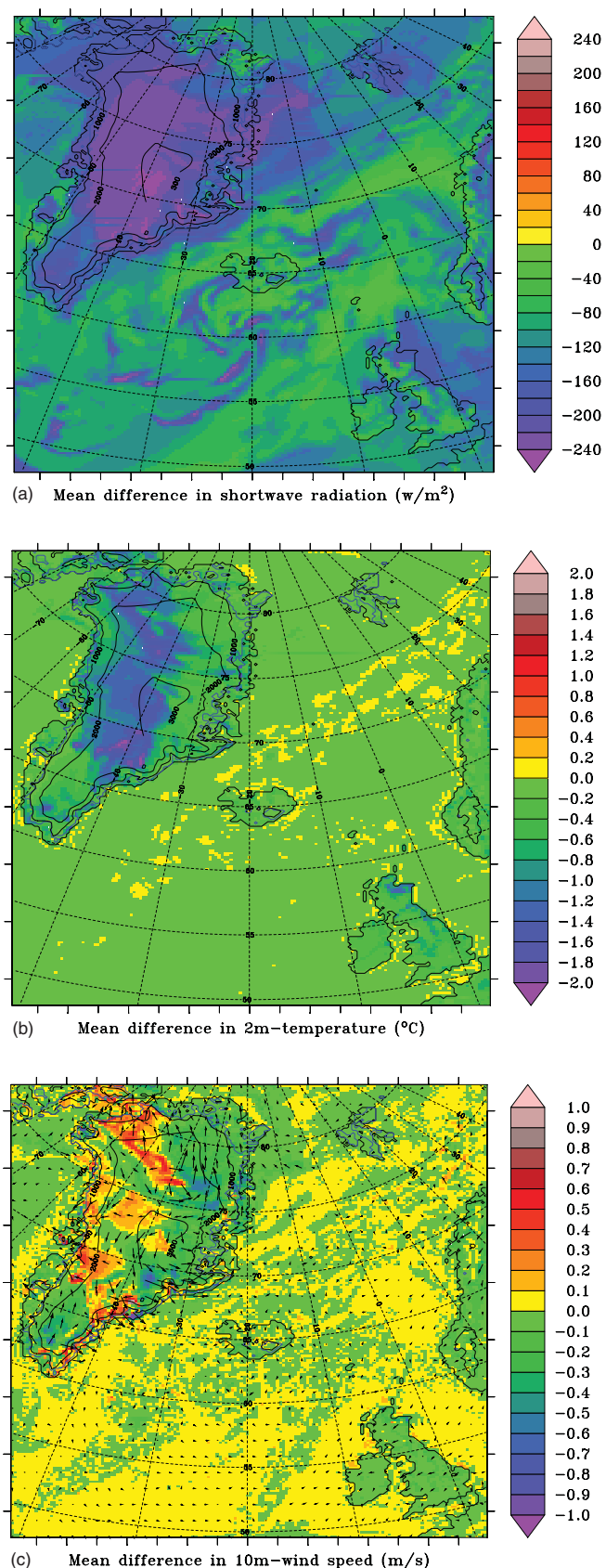
(c) Mean difference in 10m–wind speed (m/s)

Figure 13. Mean difference between simulations with and without the eclipse, obtained using the MAR regional climate model for 0930–1130 UTC on 10 June 2021: (a) downward shortwave radiation; (b) near-surface air temperature and (c) 10m wind speed.
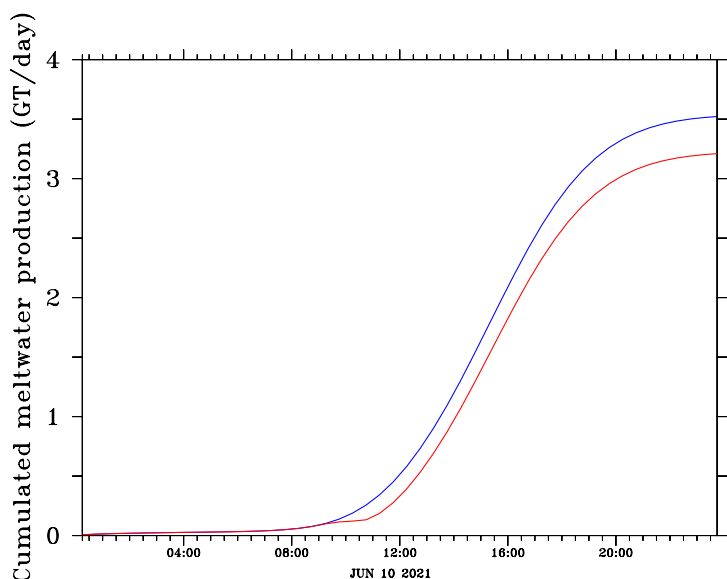
RMetS
Royal Meteorological Society

Figure 14. MAR-simulated whole Greenland Ice Sheet cumulative surface melt production (units Gt/day) integrated for 10 June 2021 with (red line) and without (blue line) the solar eclipse.
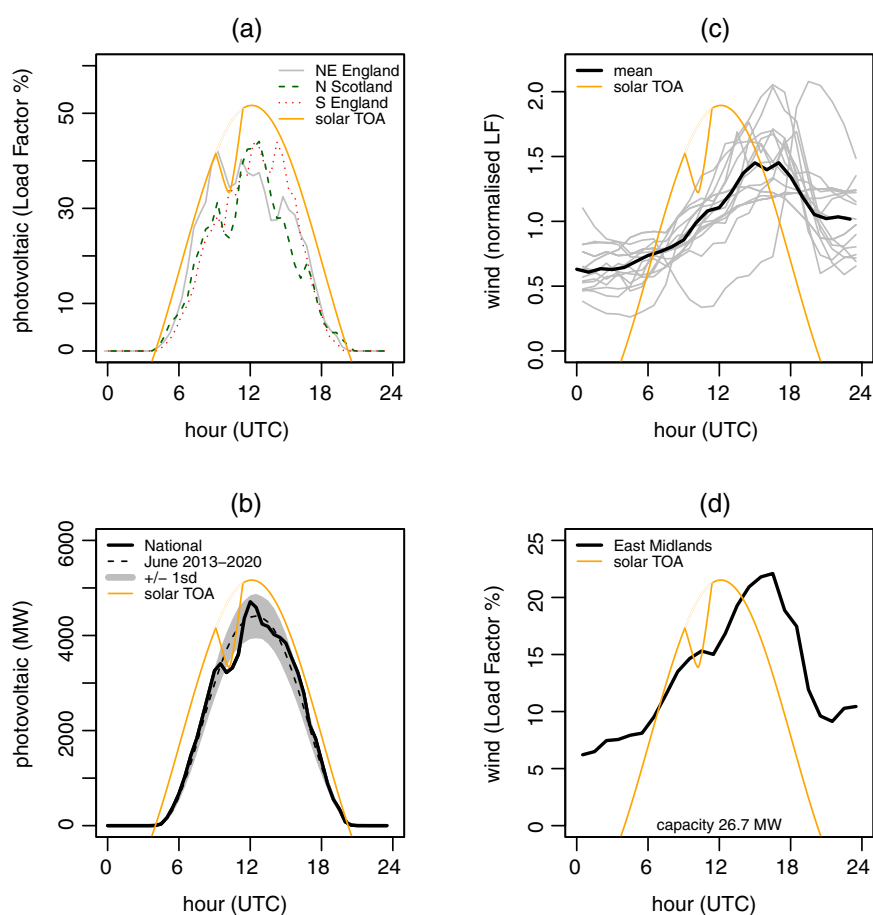

Figure 15. Effect of the 21 June 2021 partial solar eclipse on renewable energy generation. Time series of (a) photovoltaic (PV) generation in different regions, (b) national PV generation (with mean and one standard deviation for June 2013–2020), (c) wind generation across small wind turbine sites and (d) wind generation from the East Midlands. (Load factor, LF is the proportion of generating capacity.) In (c), the load factor of each turbine site has been normalised by its mean value, to allow the variability to be compared, with the mean taken of all the normalised values. In all plots, the gold curve shows top of atmosphere (TOA) solar radiation calculated (relative values, unscaled) for a horizontal surface at Birmingham on the same day, assuming a 30% eclipse).

RMetS
Royal Meteorological Society